Forelimb Treatment in a Large Cohort of Dystrophic Dogs Supports Delivery of a Recombinant AAV for Exon Skipping in Duchenne Patients

Caroline Le Guiner[1,2], Marie Montus[2], Laurent Servais[3], Yan Cherel[4], Virginie Francois[1], Jean-Laurent Thibaud[5,6], Claire Wary[5], Béatrice Matot[5], Thibaut Larcher[4], Lydie Guigand[4], Maeva Dutilleul[4], Claire Domenger[1], Marine Allais[1], Maud Beuvin[7], Amélie Moraux[8], Johanne Le Duff[1], Marie Devaux[1], Nicolas Jaulin[1], Mickaël Guilbaud[1], Virginie Latournerie[2], Philippe Veron[2], Sylvie Boutin[2], Christian Leborgne[2], Diana Desgue[2], Jack-Yves Deschamps[4,9], Sophie Moullec[9], Yves Fromes[9], Adeline Vulin[10], Richard H Smith[11], Nicolas Laroudie[2], Frédéric Barnay-Toutain[2], Christel Rivière[2], Stéphanie Bucher[2], Thanh-Hoa Le[2], Nicolas Delaunay[2], Mehdi Gasmi[2], Robert M Kotin[11], Gisèle Bonne[7,12], Oumeya Adjali[1], Carole Masurier[2], Jean-Yves Hogrel[8], Pierre Carlier[5], Philippe Moullier[1,2,13] and Thomas Voit[7]

[1]Atlantic Gene Therapies, INSERM UMR 1089, Université de Nantes, CHU de Nantes, Nantes, France; [2]Généthon, Evry, France; [3]Institut de Myologie, Service of Clinical Trials and Databases, Paris, France; [4]Atlantic Gene Therapies, INRA UMR 703, ONIRIS, Nantes, France; [5]Institut de Myologie, Laboratoire RMN, AIM & CEA, Paris, France; [6]UPR de Neurobiologie, Ecole Nationale Vétérinaire d'Alfort, Maisons Alfort, France; [7]Institut de Myologie, Groupe Hospitalier Pitié-Salpêtrière, Université Pierre and Marie Curie Paris 6 UPMC-INSERM UMR 974, CNRS FRE 3617, Paris, France; [8]Institut de Myologie, Neuromuscular Physiology and Evaluation Laboratory, Paris, France; [9]Atlantic Gene Therapies, Centre de Boisbonne, ONIRIS, Nantes, France; [10]Research Institute, Center for Gene Therapy, Nationwide Childrens Hospital, Columbus, Ohio, USA; [11]Laboratory of Molecular Virology and Gene Therapy, National Heart Lung and Blood Institute, National Institute of Health, Bethesda, Maryland, USA; [12]AP-HP, Groupe Hospitalier Pitié-Salpêtrière, U.F. Cardiogénétique et Myogénétique, Service de Biochimie Métabolique, Paris, France; [13]Department of Molecular Genetics and Microbiology, University of Florida, Gainesville, Florida, USA

Duchenne muscular dystrophy (DMD) is a severe muscle-wasting disorder caused by mutations in the dystrophin gene, without curative treatment yet available. Our study provides, for the first time, the overall safety profile and therapeutic dose of a recombinant adeno-associated virus vector, serotype 8 (rAAV8) carrying a modified U7snRNA sequence promoting exon skipping to restore a functional in-frame dystrophin transcript, and injected by locoregional transvenous perfusion of the forelimb. Eighteen Golden Retriever Muscular Dystrophy (GRMD) dogs were exposed to increasing doses of GMP-manufactured vector. Treatment was well tolerated in all, and no acute nor delayed adverse effect, including systemic and immune toxicity was detected. There was a dose relationship for the amount of exon skipping with up to 80% of myofibers expressing dystrophin at the highest dose. Similarly, histological, nuclear magnetic resonance pathological indices and strength improvement responded in a dose-dependent manner. The systematic comparison of effects using different independent methods, allowed to define a minimum threshold of dystrophin expressing fibers (>33% for structural measures and >40% for strength) under which there was no clear-cut therapeutic effect. Altogether, these results support the concept of a phase 1/2 trial of locoregional delivery into upper limbs of nonambulatory DMD patients.

Received 28 February 2014; accepted 14 July 2014; advance online publication 9 September 2014. doi:10.1038/mt.2014.151

INTRODUCTION

Duchenne muscular dystrophy (DMD) is the most frequent muscular dystrophy in childhood, affecting 1 in 3,500 to 5,000 male births. DMD is a progressive degenerative disease caused by mutations in the *dmd* gene encoding dystrophin located on the X chromosome. Dystrophin is required for the assembly of the dystrophin–glycoprotein complex, and provides a strong mechanical link between the cytoskeleton and the extracellular matrix. Absence of dystrophin results in myofiber degeneration and necrosis, progressive muscle weakness and fatigability, and finally premature death.[1] Several therapeutic approaches including antisense oligonucleotide (AO)-based exon skipping are currently investigated, but yet there is no curative treatment available for DMD.[2]

The majority of the DMD patients carry reading-frame altering mutations of the *dmd* gene resulting in loss of dystrophin expression. When a mutation maintains the reading frame and the most critical parts of the gene, a truncated but still functional dystrophin protein is expressed, leading to the less severe phenotype of Becker muscular dystrophy (BMD).[3] The selective removal of exons (*i.e.*,

The first three authors contributed equally to this work as first authors and the last two authors contributed equally to this work as senior authors.
Correspondence: *T Voit, Institut de Myologie, Groupe Hospitalier Pitié-Salpêtrière, Université Pierre and Marie Curie Paris 6 UPMC-INSERM UMR 974, CNRS FRE 3617, Paris, France. E-mail: t.voit@institut-myologie.org or P Moullier, Atlantic Gene Therapies, INSERM UMR 1089, Université de Nantes, CHU de Nantes, Nantes, France. E-mail: moullier@ufl.edu*

exon skipping) flanking an out-of frame DMD mutation can result in in-frame mRNA transcripts that may be translated into an internally deleted dystrophin protein with therapeutic activity.[4] In theory, exon skipping could rescue more than 80% of DMD patients, including those with deletion mutations, nonsense mutations and duplications. Even if single and double exon skipping has essentially been efficiently used until now, 70% of the DMD patients could be cured by multiple skipping of exons 45 to 55 in the dystrophin messenger.[5] Exon skipping can be achieved using chemically modified AOs or small nuclear RNAs (snRNAs). In both cases, sequences are designed to bind complementary sequences in the targeted mRNA, which will modify pre-mRNA splicing to correct the reading frame of a mutated transcript.[4] If a relative efficacy of chemically modified AOs was obtained in DMD patients,[6–8] a recent phase 3 clinical trial using AOs was unable to show a statistically significant clinical improvement in the treated patients compared to placebo.[9] Moreover, as AOs have short biological half-lives, they must be regularly administered and severe adverse events were observed in some instances.[7,8] An alternative approach is to clone AOs within a modified snRNA sequence, which allows a proper subcellular localization and facilitates AO inclusion into the spliceosome. The U7snRNA, a nonspliceosomal molecule that is normally involved in the processing of the 3′ end of histone mRNAs, can be engineered and redirected to the spliceosome to deliver antisense sequences.[10] Such snRNA can be packaged in recombinant adeno-associated virus (rAAV) vectors, allowing a long-lasting repair without the need for continuous administration.[11] The proof of principle of such a correction was obtained in the dystrophin-deficient *mdx* mouse and GRMD (Golden Retriever Muscular Dystrophy) dog models, after injection of rAAV1 or rAAV6 vectors carrying a specific U7snRNA expression cassette into skeletal or cardiac muscles.[12–16]

Here, we present the first study that provides the safety profile and the therapeutic index obtained in GRMD dogs and designed to translate the rAAV-U7-mediated exon skipping approach into the clinic for man. The GRMD dog is the most relevant DMD animal model due to the homology with the human disease.[17] The dystrophic phenotype results from a point mutation in the acceptor splice site of intron 6 of the canine *dmd* gene, causing skipping of exon 7 during processing of the dystrophin messenger, disruption of the reading frame and premature termination of translation.[18] Removing exons 6 through 8 restores a correct reading frame and rescues a dystrophin protein, missing 158 amino-acids in its N-terminal actin binding domain, but still functional.[13,15,16] In the GRMD model, our therapeutic product was defined as a rAAV8 vector carrying a modified U7snRNA specific for the skipping of exons 6 to 8 of the dystrophin transcript (rAAV8-U7snRNA-E6/E8). For the transduction of large muscular territories, the mode of delivery was the one intended for our future application in human, *i.e.*, the locoregional transvenous perfusion of the forearm. Several studies have shown that rAAV-mediated transduction of an entire limb was achieved by one single locoregional transvenous perfusion during which the limb is transiently isolated from the general circulation by an atraumatic tourniquet.[15,19–21] Recently, the safety profile of such a mode of delivery was further confirmed in neuromuscular disease patients receiving saline solution in the lower limb.[22] Although, treating systemic diseases such as DMD will ultimately require widespread muscle transduction including the heart and the diaphragm, we believe that until systemic administration of rAAV vector is comprehensively assessed in preclinical settings, the present locoregional delivery route to the forelimb(s) is an intermediate step indicated in nonambulatory DMD patients to maintain muscle strength and function in the forearm.

In the present study, rAAV8-U7snRNA vector was delivered to 18 juvenile GRMD dogs by locoregional transvenous injection into one forelimb. Increasing doses infused in various volumes and at different flow rates, were used (i) to define the therapeutic dose of rAAV8-U7snRNA-E6/E8, (ii) to set up the injection protocol, and (iii) to assess the safety profile of both the gene therapy vector and the mode of delivery, modeling precisely what is intended to be used in man.

RESULTS

Study design

Eighteen 3- to 4-month-old GRMD dogs were injected in one forelimb via locoregional transvenous infusion (**Table 1**), with increasing doses (from 5^E12 vg/kg to 5^E13 vg/kg) of a rAAV8-U7snRNA-E6/E8 vector. Three control GRMD dogs were also included and received the vehicle only. To set up our injection protocol on the basis of what was recently documented in patients with neuromuscular diseases,[22] the total perfusion volume was either 40 or 20% of the limb volume. Animals of group 6 received the vector at a flow rate of 35 ml/minute compared to 7–20 ml/minute for all other groups. The quality control testing of the rAAV batches used in the study is provided in **Supplementary Table S1**.

All animals were followed for ≈3.5 months postinjection before euthanasia, except for D5, D12, and D17, which had to be sacrificed between 2 and 2.5 months postinjection due to gastrointestinal disorders, frequently associated with the morbidity of this model and not related to our treatment. Indeed there was no evidence for vector toxicity at necropsy analysis and pathology examination of these three dogs.

Blood tests and clinical assessment show good safety profile of the vector upon locoregional delivery

Locoregional transvenous injection was eventless in all dogs. The venous pressure was monitored at the level of the catheter. Maximal pressures, reached few minutes after the beginning of vector delivery, were ~380 mm Hg, ~150 mm Hg, and ~280 mm Hg, when the volume of the perfusate and the flow rate were respectively 40% of the limb volume at 10–20 ml/minute, 20% of the limb volume at 10–20 ml/minute, and 20% of the limb volume at 35 ml/minute (**Table 1**).

Blood tests including electrolytes, kidney, and liver function parameters and complete hematology counts remained unchanged in the hours, days, and weeks after vector delivery. No adverse effect related to the injection and/or the product itself was noted on the clinical status of the dogs (data not shown). As a key component of the safety profile of both the delivery protocol and the gene therapy vector itself, the inflammatory cytokines interleukin IL-2, IL-4, IL-6, IL-8, IL-10, IL-15, interferon-α, and tumor necrosis factor-α were measured in the plasma, from 6 hours until 2 weeks after injection and at sacrifice. We found no significant increase of any of them compared to the preinjection levels (data not shown).

Table 1 Characteristics of the different Golden Retriever Muscular Dystrophy dogs of this study

Group	Dog	Volume % limb	Type of injection and dose	Flow rate (ml/minute)	Injected rAAV batch	Maximal line pressure (mm Hg)	Segmental limb volume (ml)	Injected volume (ml)	Injected volume (ml/kg)
Control	C1	40[b]	Buffer	19	N/A	382	/	110	12
Group 1	D1	40	rAAV8-U7-E6/E8 5^E12 vg/kg	8	STR18	381	135	54	12
	D2	40		8	STR18	361	230	105	12
Group 2	D3	40[b]	rAAV8-U7-E6/E8 1^E13 vg/kg	10	STR18	354	/	110	12
	D4	40[b]		7	STR18	353	/	81	12
	D5[a]	40		12	A.10001	300	250	99	12
Group 3	D6	40[b]	rAAV8-U7-E6/E8 5^E13 vg/kg	20	STR16	500	/	140	12
	D7	40[b]		20	A.10001.DEV	355	/	120	12
	D8	40[b]		13	STR17	416	/	105	12
Control	C2	20	Buffer	10	N/A	108	325	65	6
	C3	20		10	N/A	146	280	57	6
Group 4	D9	20	rAAV8-U7-E6/E8 1^E13 vg/kg	10	STR18	160	250	51	7
	D10	20		10	STR18	173	320	65	6.5
	D11	20		10	A.10001.DEV	124	340	69	6.5
	D12[a]	20		10	A.10001	190	310	65	7
Group 5	D13	20	rAAV8-U7-E6/E8 5^E13 vg/kg	10	A.10001.DEV	132	300	60	6
	D14	20		10	A.10002.STD	108	300	61	6
	D15	20		10	A.10001	190	310	63	6
Group 6	D16	20	rAAV8-U7-E6/E8 1^E13 vg/kg	35	STR18	300	260	47	6
	D17[a]	20		35	A.10002.DEV	300	240	42	6.5
	D18	20		35	A.10002.DEV	248	370	69	6

[a]Anticipated sacrifice. [b]Volume % limb estimated (extrapolation from the injected volume)
/, not determined.

Locoregional delivery leads to wide spread dose dependent transduction mostly below the tourniquet

Using a quantitative PCR (Q-PCR) specific for the transgene sequence, vector biodistribution was assessed at euthanasia in 13 muscles of each forelimb, as well as in several muscles at distance (total of 46 muscles) and in major organs (**Supplementary Table S2**). No Q-PCR signal was detected on whole blood at euthanasia (data not shown) confirming that vector genome detection was restricted to the tissue itself. The numbers of vg/dg (vector genome per diploid genome) in each of the rAAV-injected dogs were plotted on **Figure 1a**. As vector dose increased, the number of vg/dg proportionally increased with less than 1 copy, ~1 to ~3 copies and ~3 to ~15 copies per dg following the administration of respectively 5^E12 vg/kg, 1^E13 vg/kg, and 5^E13 vg/kg of rAAV vector. The latter including groups 3 and 5, had significantly more vg/dg as compared to the lowest two doses administered, whatever the injection volume was ($P < 0.05$). Simultaneously, the coefficient of variation (CV), which reflects the heterogeneity of the values, decreased as the vector dose increased, while injected in a large volume (40% of the limb volume). In contrast, when the perfusate was reduced to 20% of the limb volume, the CVs were higher, indicating that reducing the injected volume resulted in a less homogeneous transduction pattern. Finally, when the flow rate was increased to 35 ml/minute, neither the number of vg/dg in the injected limb nor the CV were significantly improved.

Consistent with the fact that the locoregional transvenous administration procedure cannot entirely prevent leakage beyond the tourniquet, shedding of the vector was detected after injection (**Supplementary Table S3**). In the muscles just above the tourniquet as well as in muscles at distance, the vg/dg numbers were at least one log lower than in the injected forelimb. Liver and to a lesser extent lymph nodes and spleen exhibited near-equivalent levels of vg/dg numbers to the exposed transduced forelimb (**Figure 1b**).

Skipped dystrophin messenger is present in transduced muscles

Using a specific nested RT-PCR, dystrophin messenger RNA molecules were characterized from various muscles. Irrespective of the protocol used for the injection of 1^E13 vg/kg or 5^E13 vg/kg of rAAV8-U7snRNA-E6/E8 vector, RT-PCR showed skipped dystrophin messengers lacking exons 6, 7, and 8 (**Figure 2b**,**c**). RT-PCR product identity was confirmed by sequencing (data not shown). The 5^E13 vg/kg vector dose resulted in fully skipped messenger, *i.e.*, no residual nonskipped dystrophin messenger detectable (**Figure 2c**), whereas the 1^E13 vg/kg dose resulted in partial skipping of the dystrophin messenger (**Figure 2b**). Skipping was undetectable in animals receiving the lowest dose (**Figure 2a**). In the GRMD dogs injected with the highest dose of vector, partial exon skipping was also detected in some muscles of the contralateral forelimb, in the diaphragm and occasionally in the heart

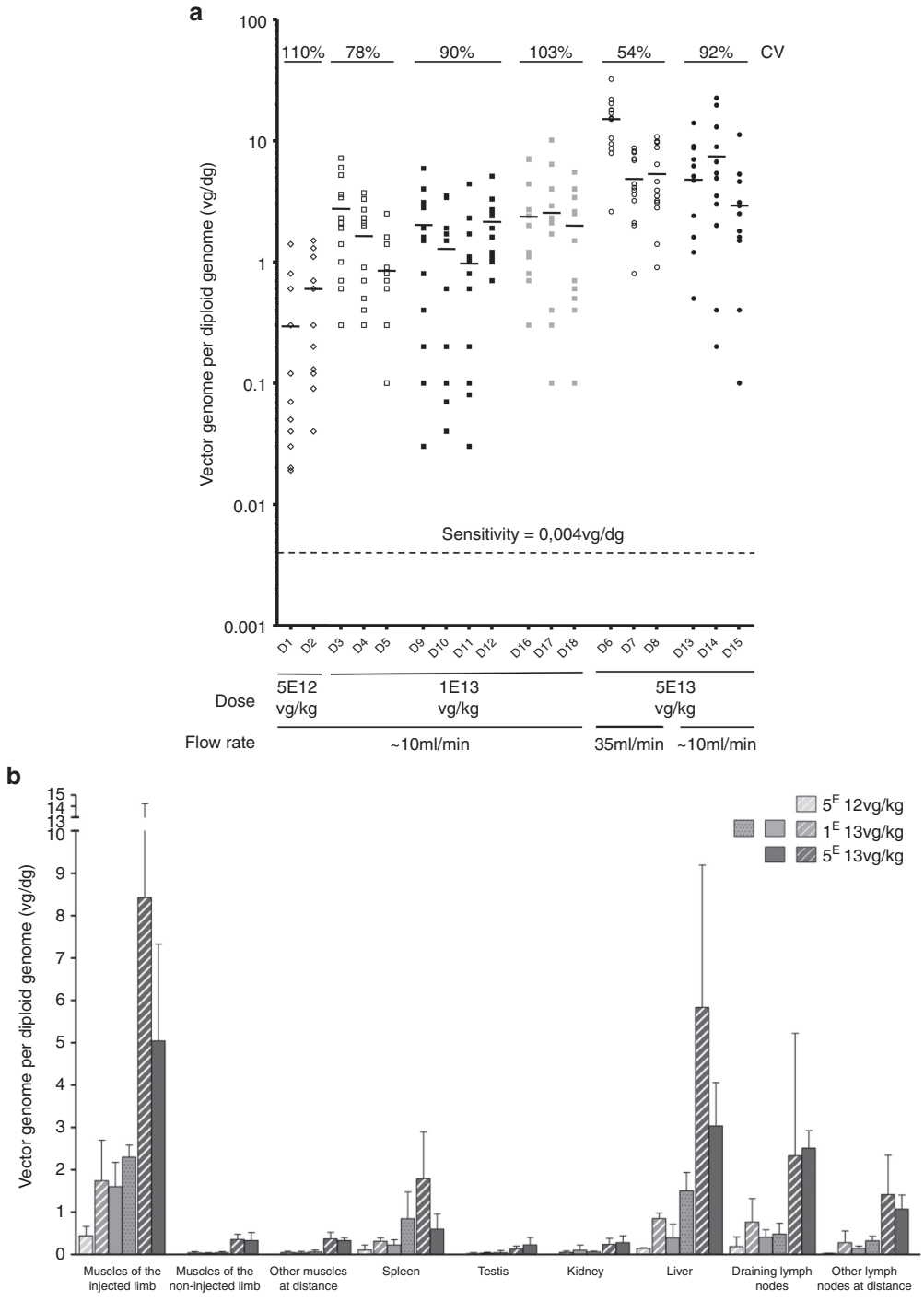

Figure 1 Vector biodistribution in the injected forelimb and at distance. (**a**) Vector copy number per diploid genome in each muscle of the injected forelimb of each rAAV-injected dog at euthanasia. A total of 13 muscles were analyzed in the injected limb. Each point represents the vector copy number per diploid genome in each muscle of the injected limb. Empty symbols were used for the groups of dogs injected with 40% of the limb volume (groups 1, 2, and 3), and full symbols were used for the groups of dogs injected with 20% of the limb volume (groups 4, 5, and 6). The small horizontal bars represent the mean of the values obtained for each dog. No signal was detected (<0.004 vg/dg) in the muscles of the control dogs. CV, coefficient of variation within the injected forelimbs. (**b**) Vector copy number per diploid genome in different tissues of the different groups of dogs at euthanasia. For each dog, the analysis was performed on 13 muscles of the injected forelimb, on 13 muscles of the noninjected forelimb, on 20 muscles at distance (muscles of hind limbs (n = 2), muscles of the body (n = 15), heart (n = 2) and diaphragm), on spleen (n = 1), on testis (n = 2), on kidney (n = 1), on liver (n = 3), on draining lymph nodes (n = 2), and on other lymph nodes at distance (n = 5). Each bar of the histogram represents the mean (with standard deviations) of the results obtained in the different dogs of a same group. Striped bars were used for the groups of dogs injected with 40% of the limb volume (groups 1, 2, and 3). Full bars were used for the groups of dogs injected with 20% of the limb volume and a flow rate of 10 ml/minute (groups 4 and 5), and punctuated bars were used for the groups of dogs injected with 20% of the limb volume and a flow rate of 35 ml/minute (group 6). No signal was detected (<0.004 vg/dg) in the tissues of the control dogs (data not shown).

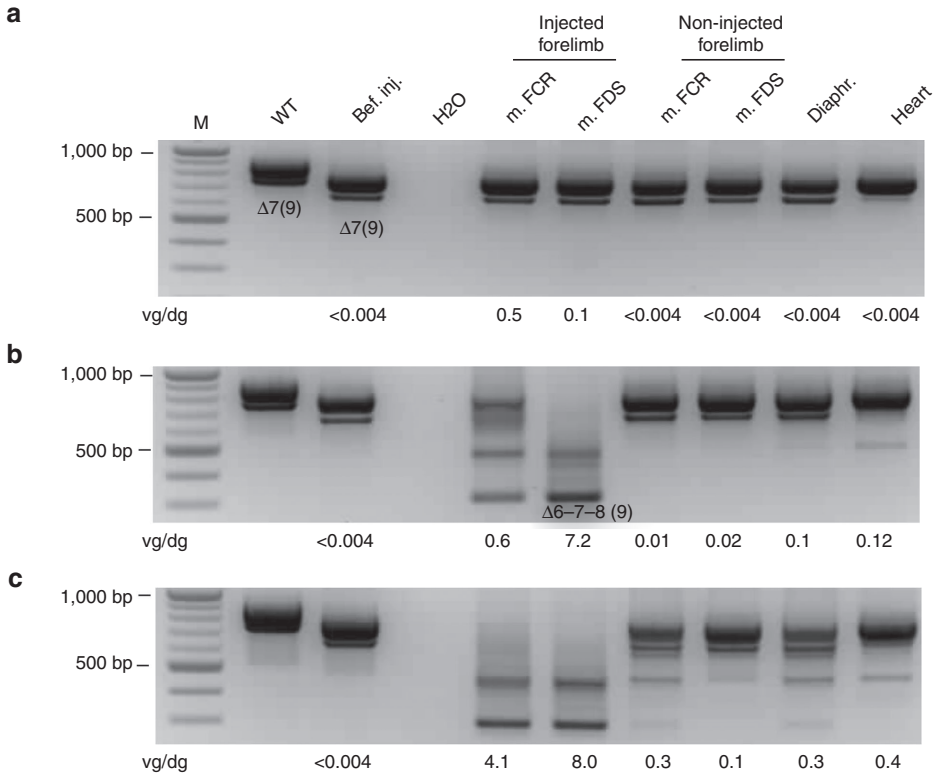

Figure 2 Dystrophin messenger analysis in muscles. Representative results are presented for one dog of each injected dose: (**a**) 5^E12 vg/kg: D1, (**b**) 1^E13 vg/kg: D3, and (**c**) 5^E13 vg/kg: D7. The dystrophin messenger was detected by nested RT-PCR from exon 3 to 10 in muscles sampled at euthanasia (m. FCR = muscle flexor carpi radialis; m. FDS = muscle flexor digitorum superficialis; diaphragm and heart). The PCR products (910 bp and 778 bp fragments) detected in healthy (WT) dog correspond to mRNA variants with or without the alternative exon 9.[50] The PCR products (791 bp and 659 bp fragments) detected in the Golden Retriever Muscular Dystrophy (GRMD) dogs before injection (bef. inj.) correspond to mRNA variants lacking either exon 7 or exons 7 and 9, respectively.[18] After injection, the two new bands (436 bp and 304 bp fragments) detected in some muscles correspond to in-frame mRNAs lacking exons 6 to 8 and 6 to 9, respectively. The copy numbers of vector genome per diploid genome detected by Q-PCR on gDNA from the same tissue sample are indicated under each panel. No skipping was detected in the muscles of the control dogs.

(**Figure 2c**). Finally and although the nested RT-PCR approach is not quantitative, there was an obvious correlation between the skipping efficiency and the number of vg/dg found in each muscle.

Dystrophin is expressed at high levels in transduced muscles

The same muscle samples processed for vg/dg determination (**Supplementary Table S2**) were used to evaluate dystrophin expression. **Figure 3a** shows representative immunofluorescence images obtained in dogs injected with the different vector doses and **Table 2** summarizes the results obtained by counting of the percentage of dystrophin positive fibers after immunoperoxidase staining. As vector dose rose, the percentage of dystrophin-positive fibers found in the perfused forelimb proportionally increased from 18% (group 1), 23, 35, and 36% (groups 4, 2, and 6) and 58 and 76% (groups 5 and 3). The high-dose groups (groups 3 and 5) had significantly higher percentages compared to the other groups ($P < 0.05$). Moreover, when the injection volume was reduced, a significant difference in levels of dystrophin-positive fibers was observed only between the two groups that had received this highest vector dose ($P < 0.05$). When GRMD dogs received the intermediate vector dose (1^E13 vg/kg) at a constant 20% limb volume, the increase of flow rate up to 35 ml/minute resulted in a significant increase in the percentage of dystrophin-positive fibers ($P < 0.05$). Consistent with the vg/dg findings described above, CVs were lower at the highest vector doses administered either in the 20 or 40% limb volume. Representative examples of the heterogeneity of dystrophin expression patterns within a same injected forelimb, correlated with the analysis of dystrophin messenger exon skipping in the same muscles, are given on **Supplementary Figure S1**. Finally, increasing the flow rate up to 35 ml/minute seemed to partially improve dystrophin-labeling homogeneity (**Table 2**). Beyond the tourniquet and at distant sites, significant levels of dystrophin-positive fibers were also found essentially in the animals that had received the highest vector dose. As shown on **Supplementary Figure S2**, the relationship between the percentage of dystrophin positive fibers and the number of vg/dg detected in each muscle of injected limbs, displayed a nice linear regression, 40% of positive fibers being detected with ≈1 vg/dg.

Of note, the majority of the dystrophin-positive fibers, showed a staining intensity, which was comparable to that observed in healthy muscle (**Figure 3a**). Along with the presence of dystrophin, components of the dystrophin-associated protein complex (*i.e.*, β-dystroglycan, β-sarcoglycan, and γ-sarcoglycan) were restored at the periphery of the muscle fibers and consistent with the dystrophin expression pattern, utrophin-staining signal was inversely proportional (data not shown). Each dog also had a western blot performed on total protein extracts from muscles of

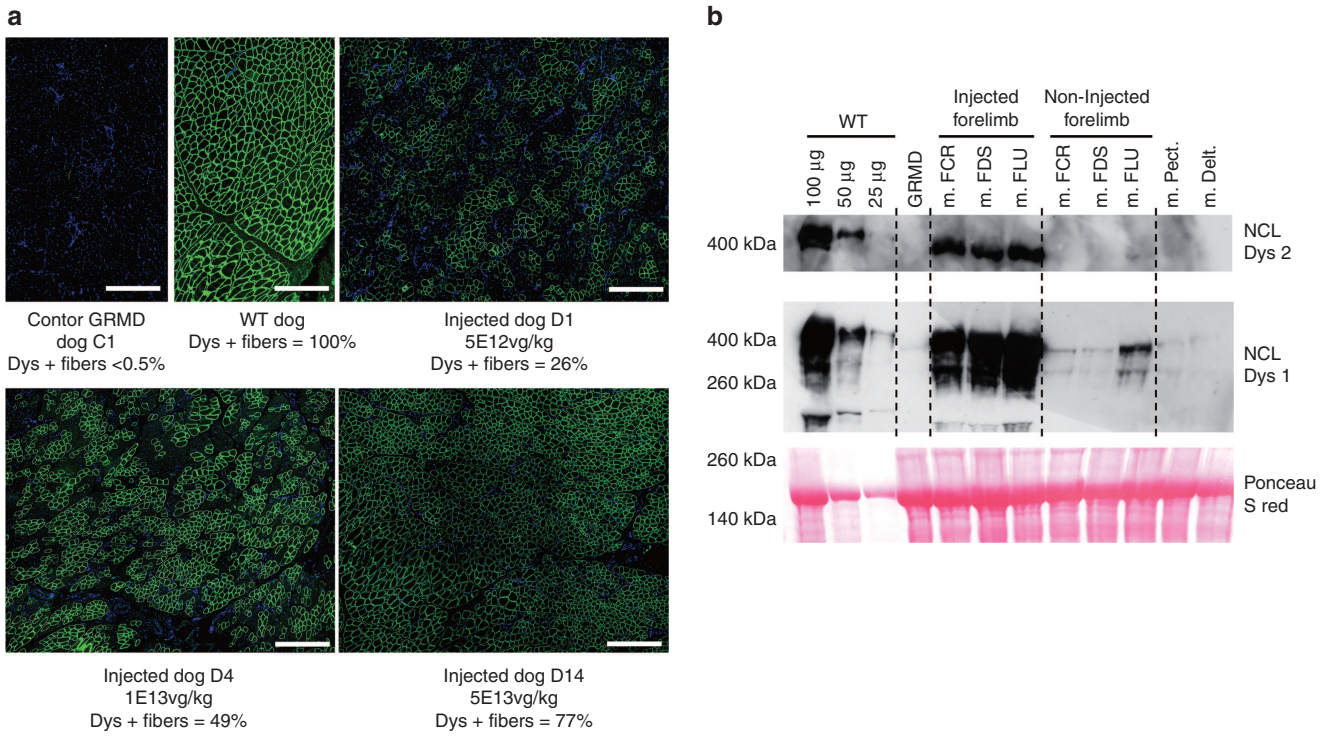

Figure 3 Analysis of dystrophin expression in muscles by immunostaining and western-blot analysis. (**a**) Dystrophin immunofluorescence (NCL-DYS2 monoclonal antibody) on transverse sections of muscle samples (muscle digitorum extensor communis) obtained at sacrifice from a healthy (WT) dog, a control Golden Retriever Muscular Dystrophy (GRMD) dog (C1) and of three GRMD dogs injected with different doses of rAAV (5^E12 vg/kg: D1. 1^E13 vg/kg: D4 and 5^E13 vg/kg: D14). Scale bar = 500 µm. (**b**) Western-blot analysis of total proteins (100 µg) extracted from muscles of dog 15 (m. FCR = muscle flexor carpi radialis; m. FDS = muscle flexor digitorum superficialis; m. FLU = muscle flexor lateralis ulnaris; m. pectoralis and m. deltoideus). The blot was stained with NCL-DYS1 or NCL-DYS2 monoclonal antibodies (the two antibodies having different levels of sensitivity) to reveal the presence of the novel ~405 kDa dystrophin band. Muscle from a control GRMD dog was used as negative control. Muscle from a healthy (WT) dog was used as positive control, and revealed the presence of the 427 kDa normal dystrophin band. Different quantities (25–100 µg) of this protein extract were loaded, to allow a semiquantification of the signals obtained in the injected dog. A Ponceau S red staining was used to validate protein loadings.

the two forelimbs. These analyses confirmed the presence of the ~405 kDa corrected dystrophin band (a representative example is provided **Figure 3b**), the intensity of which was consistent with the transduction pattern.

Improvement of muscle pathology in the transduced territories

In DMD patients and GRMD dogs, muscular lesions result from the absence of dystrophin protein. "Phase I" lesions consist of hyalinization, hypertrophy, abnormal accumulation of calcium salts, necrosis, macrophage, and lymphocyte infiltration and subsequent regeneration of myofibers. "Phase II" lesions are fibrosis and general myofiber diameter heterogeneity. Beyond that stage, adiposis takes place essentially in DMD patients and to a lesser extent in GRMD dogs.[23,24] Using morphometric analyses, we analyzed two anatomically opposed muscles within the perfused forelimb: the flexor carpi ulnaris muscle and the extensor carpi radialis muscle. In order to detect a possible relationship between gene transfer efficacy and the tissue pathology criteria, data were collected and analyzed after allotments of the muscles based on the percentage of dystrophin-positive fibers. At euthanasia, transduced muscles showed a decrease of myofiber regeneration, which was correlated with the percentage of dystrophin-positive fibers and was significant as soon as more than 33% of myofibers were expressing dystrophin ($P < 0.05$) (**Figure 4a**). In addition, a significant decrease of endomysial and total fibrosis was observed in the muscles presenting more than 33% of dystrophin-positive fibers ($P < 0.05$) (**Figure 4b,c**). However, no statistical difference was noted regarding the accumulation of calcium salts, anysocytosis, macrophage infiltration, and T and B lymphocyte infiltration (data not shown). Altogether, these results indicated that "Phase I" and "Phase II" tissue lesions are decreased in successfully transduced muscles harboring at least 33% of dystrophin-positive fibers.

Improvement of NMR imaging and spectroscopy indices within the transduced muscle territories

Proton (^{1}H) NMR imaging and phosphorous (^{31}P) spectroscopy analysis of both forelimbs were performed just prior to euthanasia in 16 of our experimental dogs (5 of them being unable to support the anesthesia required for this exam). The most relevant NMR imaging indices relying on T2, T1, and proton density weighted image signal intensities (T2w, T1w, PD) were calculated on three different muscles. The T2w/PD and T2w/T1w ratios reflect the presence of edema, inflammation, necrosis, and cell damage. The T2w heterogeneity reflects tissue disorganization and abnormal Gadolinium uptake correlates with fibrosis, necrosis and cell damage.[25] In ^{31}P spectroscopy, signals were measured from the two extensor carpi radialis muscles. Selected ratios were

Table 2 Levels of dystrophin positives fibers found within the muscles after immunostaining analysis (NCL-DYS2 monoclonal antibody)

			Injected forelimb				Noninjected forelimb	Other muscles at distance	Diaphragm
Group	Type of injection	Dog	Mean of Dys+ fibers	*CV*	Mean of Dys+ fibers for the group	*CV for the group*	Mean of Dys+ fibers	Mean of Dys+ fibers	Mean of Dys+ fibers
Control	40% of the limb	C1	<0.5%	*N/A*	<0.5%	*N/A*	<0.5%	<0.5%	<0.5%
Group 1	5^E12 vg/kg 40% of the limb	D1	13%	*128.5%*	18%	*35.4%*	<0.5%	<0.5%	1%
		D2	22%	*78.2%*			<0.5%	<0.5%	<0.5%
Group 2	1^E13 vg/kg 40% of the limb	D3	47%	*52.8%*	35%	*37.7%*	<0.5%	1%	1%
		D4	36%	*79.3%*			<0.5%	<0.5%	6%
		D5	22%	*82.5%*			4%	10%	1%
Group 3	5^E13 vg/kg 40% of the limb	D6	84%	*7.9%*	76%	*10.5%*	12%	27%	26%
		D7	77%	*20.7%*			6%	21%	19%
		D8	68%	*23.2%*			11%	12%	9%
Control	20% of the limb	C2	<0.5%	*N/A*	<0.5%	*N/A*	<0.5%	<0.5%	<0.5%
		C3	<0.5%	*N/A*			<0.5%	<0.5%	<0.5%
Group 4	1^E13 vg/kg 20% of the limb	D9	35%	*78.0%*	23%	*93.3%*	<0.5%	<0.5%	<0.5%
		D10	28%	*98.2%*			<0.5%	<0.5%	<0.5%
		D11	14%	*128.0%*			<0.5%	<0.5%	<0.5%
		D12	17%	*88.9%*			<0.5%	8%	1%
Group 5	5^E13 vg/kg 20% of the limb	D13	47%	*67.3%*	58%	*24.6%*	2%	5%	9%
		D14	72%	*26.1%*			12%	23%	42%
		D15	55%	*50.0%*			4%	5%	20%
Group 6	1^E13 vg/kg 20% of the limb 35 ml/min	D16	51%	*51.7%*	36%	*48.1%*	<0.5%	<0.5%	<0.5%
		D17	17%	*87.1%*			/	/	/
		D18	41%	*51.1%*			<0.5%	<0.5%	1%

CV, coefficient of variation; N/A, not applicable; /, not determined.

phosphodiesters to adenosine triphosphate (PDE/ATP), which reflects membrane metabolism and phosphocreatine to ATP (PCr/ATP), which characterizes metabolically active muscle tissue. Both were combined as PDE/PCr, a single sensitive index for membrane metabolism analysis.[26] Except for group 1, the injected forelimb was systematically identified from simple visual examination of NMR images, for which muscle signals were less hyper intense on T2w images and more homogeneous within and between muscles (**Figure 5a**). Observation of PCr increase and PDE decrease in ^{31}P NMR spectra (**Figure 5b**) also enabled recognition of the injected forelimb in all groups, except for group 1. As illustrated for the T2w/T1w NMR imaging index found in groups 4 and 5 compared to reference populations (**Figure 5c**) and for the NMR spectroscopic index PDE/PCr (**Figure 5d**), most indices showed an improvement in the injected forelimb as compared to the noninjected one. The high vector dose (groups 3 and 5) and the intermediate dose treated by the 40% volume injection protocol (group 2) decreased most indices to levels close to or within normal ranges of healthy dogs, while more scattered results were obtained in the animals with the lower volume of injection (groups 4 and 6). Finally, almost all NMR imaging indices remained within the pathological range in the animals of the low vector dose group (group 1). Moreover, consistent with the expression of dystrophin found in the contralateral forelimb of some dogs, several indices were also diminished in the muscles of the contralateral limb in the high dose groups (data not shown). Altogether, our results indicated that NMR and spectroscopic parameters are successfully improved in the transduced muscles of animals of groups 2, 3, and 5, *i.e.*, harboring at least ~35% of dystrophin-positive fibers (see **Table 2**).

Improvement of muscle strength in the transduced muscle territories

The functional status of the two forelimbs was evaluated by measurement of the flexion and extension strengths of the wrist, using a custom-made torque measurement device. Three measurements were done along the protocol on each of the 21 experimental GRMD dogs: before injection, ~1.5 months postinjection, and ~3 months postinjection. For each time point, the maximal torque was expressed as a percentage of predicted values computed using a model based on control values with respect to the animal weight. The maximal torque was most of the time attained at a stimulation frequency of 133 Hz (data not shown). The relative slope over the three measurements was used as an indicator of strength change for each function and each forelimb. A relationship between gene transfer efficacy and functional improvement was shown by plotting the strength changes against the percentage of dystrophin-positive fibers measured in the stimulated muscles,

the allotments having been specifically adapted to this analysis. **Figure 6** shows that when the percentage of dystrophin-positive fibers was above 40%, a significant improvement of strength was detected ($P < 0.05$).

Lack of immune response toward dystrophin

Despite an obvious and sustained therapeutic effect of rAAV8-U7snRNA-E6/E8 vector over the study period, we searched for humoral and cellular immune reactions against the newly synthetized dystrophin protein. The detection of anti-dystrophin IgG was performed by western-blot analysis on sera obtained before injection, at 1, 2, and ~3.5 months postinjection. No anti-dystrophin IgG was detected in any of the 18 rAAV-injected GRMDs indicating that, within the limits of our assay sensitivity, no humoral response towards the therapeutic protein was developed (a representative example obtained from dog D10 is provided on **Supplementary Figure S3**). Using two different protocols of antigenic lymphocyte stimulation (see **Supplementary Materials and Methods**), T cell responses directed against the novel dystrophin protein were assessed by IFN-γ ELISPOT assay using PBMC collected at different time points postinjection and splenocytes collected at euthanasia. Again, none of the analyzed experimental GRMD dogs exhibited a detectable IFN-γ response (**Supplementary Table S4**). We also monitored the anti-AAV8 capsid immune reaction and obtained classical anti IgM and IgG responses (**Supplementary Figure S4a**). Simultaneously, all rAAV-injected dogs rapidly developed dose-dependent anti-AAV8 neutralizing factors (NAF) (**Supplementary Figure S4b**). Finally, no IFN-γ response to the AAV8 capsid was detected at any time point in any analyzed dog (**Supplementary Table S4**).

DISCUSSION

The present study intended to support a future clinical trial of rAAV8-U7snRNA-based gene therapy in nonambulant DMD patients by determining the safety profile and therapeutic index of the locoregional drug delivery approach, testing different doses, optimizing the injection protocol, evaluating the concomitant risks, and monitoring immunological responses both to the vector and the dystrophin produced. Dystrophin correction using a rAAV-U7snRNA vector was previously established in DMD mouse[12,14] and dog[13,15,16] models, after local injection in skeletal muscle or heart. Beyond this stage of proof of principle, we conducted a comprehensive and systematic translational investigation in a large cohort of GRMD dogs, a clinically relevant model of DMD, and using a GMP-compliant manufactured vector following methods suitable for human trials. All dogs were injected at the age of 3–4 months, an age when clinical signs and several histological lesions due to the absence of dystrophin protein are systematically found. "Phase I" lesions (hyalinization, hypertrophy, calcification, necrosis, and regeneration) are established and some "Phase II" lesions (endomysial fibrosis and myofiber diameter heterogeneity) are often detected.[23]

The first major finding was that the mode of delivery and the gene therapy vector were both safe and therapeutic. The reassuring safety profile was consistent with the recent report of such procedure applied to neuromuscular disease patients receiving only saline solution in the lower limb.[22]

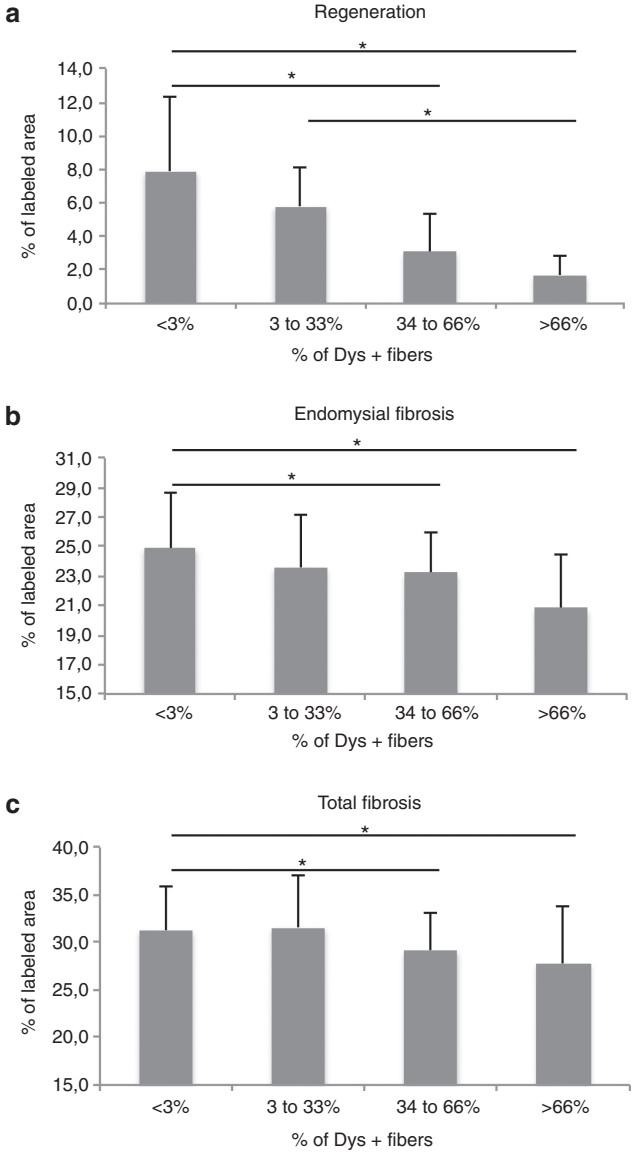

Figure 4 Improvement of pathological pattern in the dystrophin-expressing muscles. Two muscles per dog were analyzed (the flexor carpi ulnaris muscle and the extensor carpi radialis muscle) according to their percentage of Dys+ positive fibers: <3% ($n = 38$), between 3 and 33% ($n = 8$), between 34 and 66% ($n = 18$) and >66% ($n = 12$). *$P <$ 0.05. (**a**) Evaluation of myofiber regeneration. Regeneration was quantified by immunohistochemical staining of myotubes using an antibody specific for developmental myosin heavy chain isoform and automatic measurement of the percentage of the labeled area. (**b**) Evaluation of endomysial fibrosis in the muscles. Endomysial fibrosis was quantified by immunohistochemical revelation of collagen I, and automatic measurement of the percentage of the labeled area after selection of regions of interest. (**c**) Evaluation of total fibrosis in the muscles. Total fibrosis was quantified by immunohistochemical revelation of collagen I, and automatic measurement of the percentage of the labeled area.

Moreover, gene transfer and therapeutic efficacy showed tight correlations between: (i) the injected dose, (ii) the copy number of transgene in target tissue, (iii) the detection of skipped dystrophin messenger, and (iv) the level of dystrophin protein expression which corresponded to graded responses in: (v) the improvement of the local pathological pattern, (vi) the quantified NMR and ^{31}P spectroscopy parameters, and (vii) the strength of the limb. We

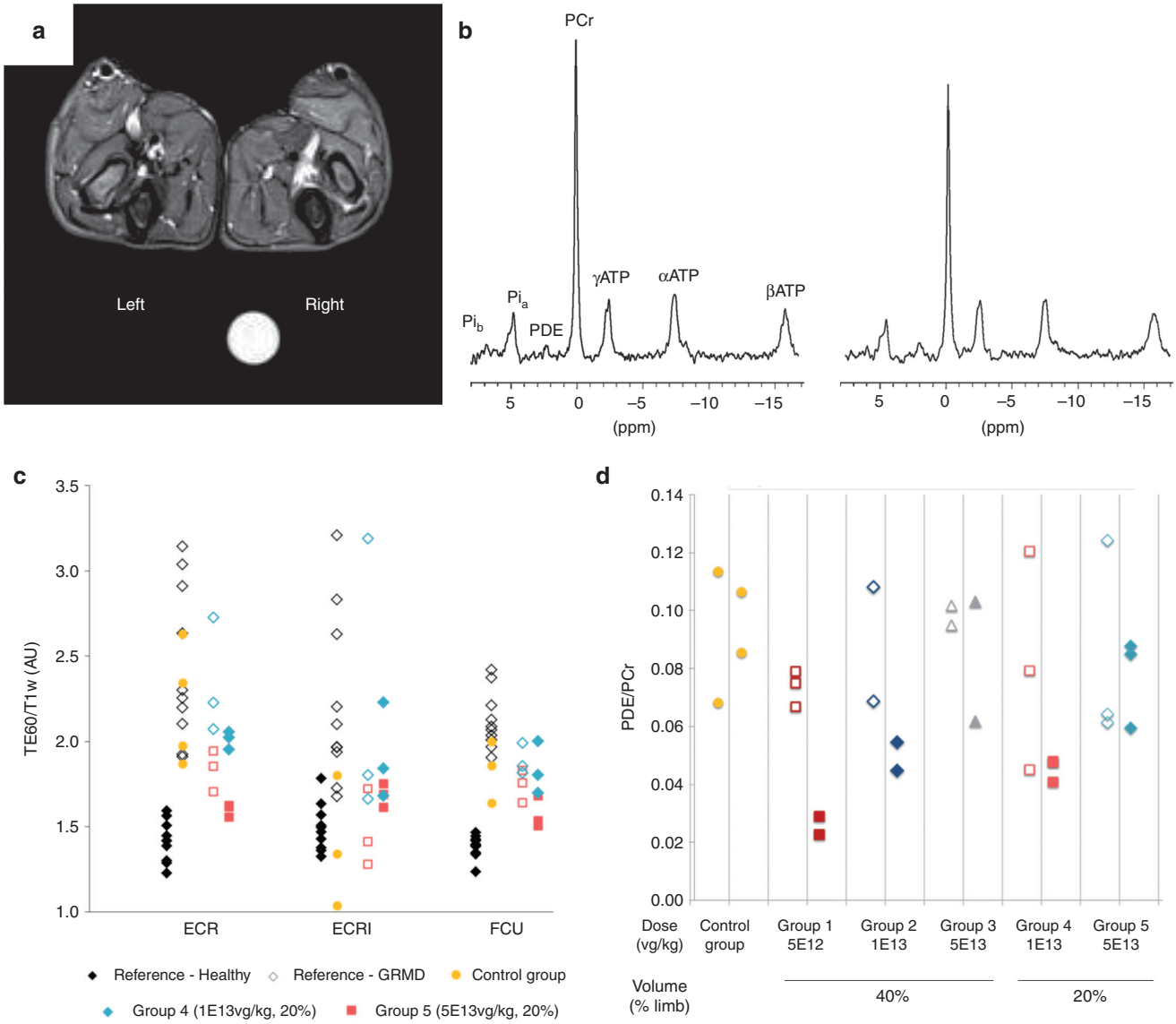

Figure 5 NMR imaging and spectroscopy analyses of muscles. (**a**) Representative example of transverse fat-saturated T2-weighted NMR image of the two forelimbs of one dog of group 3 (D8). The vector was injected in the left forelimb and imaging was performed 3 months after injection. Signal muscle intensities were decreased and more homogeneous in the injected forelimb (left) compared to the noninjected one (right). (**b**) Representative example of ^{31}P NMR spectra of the injected (left) and noninjected forelimb (right) of the same dog (D8). Phosphocreatine (PCr) was increased and phosphodiesters (PDE) were decreased relative to ATP in the treated forelimb compared to the untreated forelimb. (**c**) NMR imaging T2w/T1w muscle signal ratios of dogs injected with a small volume (20% of the limb volume), obtained from three different muscles. ECR, extensor carpi radialis brevis; ECRl, extensor carpi radialis longus; FCU, flexor carpi ulnaris). The values of this index in the injected limbs (red closed symbols for high dose and blue closed symbols for intermediate dose) were decreased compared to the noninjected ones (open red and blue symbols) and controls (yellow symbols) or nontreated Golden Retriever Muscular Dystrophy (GRMD) reference population (white symbols), and they were closer to the normal dog indices (black symbols). (**d**) NMR spectroscopy PDE/PCr muscle signal ratios of the dogs injected with high (red symbols), intermediate (blue symbols) and low vector doses (grey symbols), with large volume (40% of the limb volume) or small volume (20% of the limb volume) as compared to GRMD controls.

showed robust expression of the dystrophin protein in all muscles of the injected limb with staining intensity similar to healthy control muscle. Such intense dystrophin expression was never observed when using chemically modified AOs for the correction of dystrophin messenger by exon skipping. Indeed, in clinical trials, a maximum of 15% of normal dystrophin levels were obtained after systemic injection of AOs.[6–8] This difference in efficacy might be attributed to the difference of the reaction, which is intrinsically dependent on the nature of the skipped exon(s). But in dystrophic dogs injected with AOs designed for the skipping of exons 6 and 8 (as in our study), only 20–26% of normal dystrophin levels were found in the injected muscles even if doses several fold higher than in human trials were applied.[27,28] We think that the permanent expression of the antisense explains the power of the rAAV-U7snRNA construct compared to AOs, which have a short half-life and must be regularly readministered.

Our study allowed the definition of thresholds of efficacy, at least within the GRMD context and with this specific exon-skipping reaction. Independent methods such as muscle morphology, NMR imaging and spectroscopy, and isometric muscle

testing, which all measured distinct events, demonstrated similar improvement with comparable thresholds of dystrophin expressing fibers (>33% for structural measures and >40% for strength). These data are in correlation with the fact than in BMD and X-linked dilated cardiomyopathy patients, dystrophin levels respectively above 40% or comprised between 29 and 57% of the normal levels are sufficient to avoid muscle weakness.[29,30] In transgenic or AON-treated mdx mice, previous studies demonstrated that lower levels (~20–30%) of dystrophin expressing fibers can improve pathology and performance, and protect muscles from contraction-induced injury, but are insufficient to restore force production in skeletal muscles.[31,32] The fact that our therapeutic index is higher in GRMD dogs could be explained by the less severe muscle pathology of mdx mice compared to those of GRMD dogs.[33]

When injecting 40% of the limb volume, our therapeutic index was obtained after injection of $1^{E}13$ vg/kg. However, buffer injection of >20% of the lower limb volume may result in transient elevation of muscle compartment pressures in neuromuscular disease patients,[22] which in turn will likely be the upper safety boundary for locoregional rAAV delivery. The fact that GRMD dogs tolerated the injection of a larger volume than patients can be explained by the structural relationship of skin to underlying tissues, which differs considerably between human and dogs. And to compensate for the reduced perfusion volume, the actual therapeutic dose was $5^{E}13$ vg/kg to reach at least 40% of dystrophin-positive fibers in GRMD dogs. Because the exon-skipping reaction is sequence specific, we cannot predict the actual translation of these results into the human context, in which other antisense sequences will be used to target different exonic mutations resulting in different corrected dystrophins in different patients.

The noticeable efficacy of the exon skipping reaction coupled with the rAAV8 approach was determined after ~3.5 months of follow-up. An open topic of debate is the therapeutic stability over time. If in the context of a healthy muscle, rAAV-mediated transgene expression is stable for many years after one single intramuscular injection both in large animal models[20,34] and in a hemophilia B patient,[11] the expression stability in a pathological context such as in dystrophic muscles seems to be less evident.[35] Recent results in the mdx and dystrophin–utrophin dKO mice indicated that successful gene therapy of the dystrophic process itself is crucial for maintaining viral genome stability in transduced fibers.[36] Indeed, the DMD pathological context, if not arrested, may favor: (i) a progressive destruction of the myofibers with simultaneous elimination of the rAAV genomes; (ii) a high level of regeneration of the myofibers that could dilute the rAAV genomes, which predominantly persist as non integrated molecules in muscle cell nuclei[37]; (iii) a refractory environment due to genomic instability of the muscle cells with widespread DNA double-strand breaks and activation of the DNA damage response pathway[38]; and (iv) abnormal patterns of epigenetic regulations secondary to oxidative stress,[39] which could negatively impact on the level of expression of the therapeutic transgene. A recent study in which one GRMD dog was injected with a rAAV1-U7snRNA-E6/E8 vector and exceptionally followed for 5 years, showed a progressive decline in the number of dystrophin-positive fibers concomitant

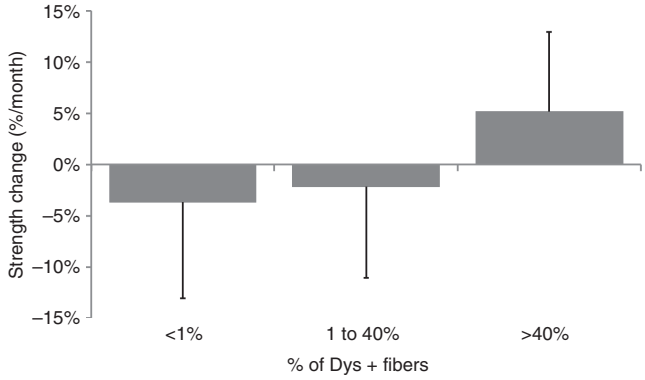

Figure 6 Relative strength changes over the protocol time in the tested forelimb, related to dystrophin expression in the stimulated muscles. The tested forelimbs were classified according to their level of dystrophin-positive fibers: less than 1% (n = 30), 1–40% (n = 21), and more than 40% (n = 14).

with the number of vg/dg in two injected muscles.[15] This decline was drastic during the first year postinjection. In our study, even if the follow up was shorter, such transgene expression decline with time was not seen, *i.e.*, no significant (*t*-test) difference was seen in the levels of dystrophin-positive fibers and vg/dg both obtained from a total of 28 muscular biopsies done in the whole cohort of dogs ~1.5 months postinjection in the injected forelimb and in the same muscles sampled at ~3.5 months postinjection. Moreover, in three additional GRMD dogs injected with the therapeutic dose of our vector and followed up to 7 months postinjection, we found similar levels of dystrophin-positive fibers and of vg/dg to those obtained in the dogs injected under the same conditions but followed ~3.5 months (Le Guiner *et al.*, unpublished data). In the study by Vulin *et al.*,[15] the fact that analyses were done on several iterative muscular biopsies could explain the difference with the present results, as iterative biopsies can promote muscle regeneration and the loss of vector genomes. The fact that the dog studied by Vulin *et al.*[15] was injected at 5–6 months of age, when "Phase II" muscular lesions can be extended (especially fibrosis), could also explain this difference. Indeed, even in mice, it was recently shown that the therapeutic efficacy of an exon skipping treatment depends on severity of the disease at the time of the treatment started.[40] The fact that we have reached a reversion of "Phase I" but also "Phase II" muscular lesions in the large majority of our dogs also supports, as in the mouse models,[36] the scenario by which reaching a therapeutic threshold with a substantial reversion of the muscular pathological pattern is a corner stone to obtain long-term rAAV genome stability in a dystrophic muscle.

The third major observation consistent with the stability of transgene expression is the lack of humoral and cellular immunity against the newly expressed dystrophin despite the occurrence of an immune response against the AAV8 capsid. Even if the rAAV vector was detectable in the periphery in GRMD dogs, systemic markers of inflammation were not detected regardless of the vector dose. Several favorable factors can explain this important observation made in fully immunocompetent dogs: (i) unlike the intramuscular injection, the locoregional transvenous injection is associated with a lack of immunotoxicity[41,42]; (ii) exon skipping therapy as opposed to dystrophin expression from a cDNA has the unique privilege

to avoid expression of the dystrophin in antigen presenting cells and thus preserves the endogenous regulation of the messenger in the relevant cell targets; and (iii) the presence of natural dystrophin "revertant fibers" in GRMD dogs (as in the majority of DMD patients)[43] is potentially a powerful tolerogenic factor. However, the latter remains a matter of debate since anti-dystrophin immunity was reported in some Duchenne patients.[44,45] Although liver was found transduced in our GRMD dogs, a tolerogenic mechanism was excluded since there was no evidence for dystrophin messenger skipping in this organ (Domenger *et al.*, unpublished data).

In conclusion, our data support the overall safety and therapeutic efficacy in GRMD dogs of locoregional intravenous injection of a rAAV8-U7snRNA at a dose of $5^{E}13$ vg/kg to reach at least 40% of dystrophin-positive fibers, paving the way for a human trial of the upper limb of nonambulatory DMD patients.

MATERIALS AND METHODS

Vector design and production. Our vector contained two modified murine U7snRNA expression cassettes with antisense sequences targeting exon splicing enhancers (ESE) in exons 6 and 8 of the canine dystrophin mRNA, each being under the control of the natural murine U7snRNA promoter. These two cassettes were previously cloned in tandem into an AAV2 vector backbone.[15] Seven pseudotyped rAAV2/8-U7nRNA-E6/E8 vector batches were produced using the Sf9/Baculovirus expression vector system,[46] adapted here for rAAV8. Briefly, Sf9 cells were grown in 50-l disposable bioreactors (Sartorius, Aubagne, France) in serum-free insect cell medium (Sf-900 II SFM medium, Life Technologies, Saint-Aubin, France) at 27 °C. When the cell concentration reached one million per milliliters, cells were transduced with Rep2-Cap8 and ITR-U7snRNA-E6/E8 Baculoviruses. Cells were grown and finally disrupted by chemical lysis to release vectors into the supernatant. The lysate was then clarified on a 0.45 µm glass fiber frontal filter (Pall, Saint-Germain-en-Laye, France) prior purification on an immunoaffinity chromatography column (AVB Sepharose HP, GE Healthcare, Velizy-Villacoublay, France). Finally, the vector was concentrated, formulated in Ringer-Lactate solution (Baxter, Maurepas, France), and sterile filtered and aliquoted by 2 ml prior freezing at −70 °C. Several quality controls tests were performed on each batch of vector (**Supplementary Table S1**). The stability of our vector at −70 °C was demonstrated over a period of 30 months, sufficient to cover the duration of our study.

Animals and vector delivery protocol. Twenty-one affected GRMD male dogs were used in this study. They were obtained from the Centre d'Elevage du Domaine des Souches (Mezilles, France) or from the Boisbonne Center for Gene Therapy (ONIRIS, Atlantic Gene Therapies, Nantes, France), two breeding centers of the same colony. They were handled and housed in the Boisbonne Center for Gene Therapy. The Institutional Animal Care and Use Committee of the Région des Pays de la Loire (University of Angers, France) approved the protocol. AAV8 seronegative animals were injected at the age of 3–4 months. The protocol was performed without any immunosuppressive regimen.

For locoregional transvenous injection, anesthesia was induced with ketamine (Imalgene 1000, Merial, Toulouse, France) in combination with diazepam (Valium, Roche, Boulogne-Billancourt, France) and was maintained using an inhalational mixture of isoflurane (Vetflurane, Virbac, Magny-en-Vexin, France) and oxygen. Analgesia was performed with morphine. A preinjection muscular biopsy was performed surgically in a biceps femoris muscle. After measurement of the limb segmental volume by water immersion, anesthetized dogs underwent cannulation of the cephalic vein with a 20-gauge catheter (B-Braun, Boulogne-Billancourt, France). Then, the forelimb was exsanguinated by applying an Esmarch bandage (Microtek Medical, Zutphen, Netherlands) and a pneumatic tourniquet (Dessillon-Dutrillaux, Castelculier, France) was placed above the elbow of the animal and inflated to 310 mm Hg to prevent any circulation in the limb. After removal of the Esmarch bandage, the perfusate (Ringer-Lactate solution alone, Aguettant, Lyon, France, or rAAV diluted in Ringer-Lactate solution) was injected. For the dogs injected with a volume corresponding to 40% of the limb volume, a final volume of 12 ml of perfusate per kg of body weight was injected using an infusion bag inflated to 300 mm Hg (Smiths Medical France, Rungis, France). For the dogs injected with a volume corresponding to 20% of the limb volume, a final volume of 6–7 ml of perfusate per kg of body weight was injected using a volumetric pump (Fresenius Vial, Brezins, France), at a fixed flow rate of 10 ml/minute or 35 ml/minute. All along the procedure, the venous pressure at the level of the catheter was monitored. After injection, the tourniquet was left in place for 15 minutes and then released. The total duration of ischemia was about 30–40 minutes. To limit discomfort of the animal due to preinjection surgical biopsy, meloxicam (Metacam, Boehringer-Ingelheim, Paris, France) was administered on the day of injection and for the following 2 days.

Euthanasia was performed by intravenous injection of pentobarbital sodium (Dolethal, Vetoquinol, Paris, France).

Vector biodistribution and vector shedding analysis. All samples were obtained in conditions to minimize cross contamination and avoid Q-PCR inhibition, as previously described.[47] Extraction of genomic DNA (gDNA) from tissues was done using the Gentra Puregene kit (Qiagen, Courtaboeuf, France) and TissueLyser II (Qiagen). Extraction of rAAV DNA from fluids was done using the Qiamp Viral RNA mini-kit (Qiagen). rAAV was extracted from 140 µl of serum. This extraction protocol was validated by spiking different doses of vector stock in the fluids, prior to the extraction. The final recovery of vector genomes was of 70% in urine and 10% in serum. Q-PCR analyses were conducted on a StepOne Plus (Life Technologies) using 50 ng of gDNA or 10 µl of fluid-extracts, in duplicates. All reactions were performed in a final volume of 25 µl containing template DNA, Premix Ex taq (Ozyme, Saint-Quentin-en Yvelines, France), 0.4 µl of ROX reference dye (Ozyme), 0.2 µmol/l of each primer (Life Technologies), and 0.1 µmol/l of Taqman probe (Life Technologies). Vector copy numbers were determined using primers and probe designed to specifically amplify the region between the two U7 snRNA expression cassettes (forward: 5′-CAGCCAATCACAGCTCCTATGTT-3′; reverse: 5′-GCTTTGATCCTTCTCTGGTTTCC-3′; probe: 5′-FAM-CCA TGCTCTAGCCACATACGCGTTTCC-TAMRA-3′). Endogenous gDNA copy numbers were determined using primers and probe designed to amplify the canine β-glucuronidase gene (forward: 5′-ACGCTG ATTGCTCACACCAA-3′; reverse: 5′-CCCCAGGTCTGCTTCATAGTT G-3′; probe: 5′-FAM-CCCGGCCCGTGACCTTTGTGA-TAMRA-3′). For each sample, C_t values were compared with those obtained with different dilutions of linearized standard plasmids (containing either the U7 snRNA expression cassettes or the canine β-glucuronidase gene). The absence of Q-PCR inhibition in the presence of gDNA was checked by analyzing 50 ng of gDNA extracted from tissues samples or 10 µl of fluid extract from a control animal, spiked with different dilutions of standard plasmid. Results were expressed in vector genome per diploid genome (vg/dg). The sensitivity of our test was 0.004 vg/dg. For fluids, only the transgene specific Q-PCR was performed and results were expressed in vector genome (vg) per ml of fluid extracted. The sensitivity was 50 vg in 10 µl of fluid extract. Statistical analyses were performed using a Fischer's least significant difference test after two-way analysis of variance (ANOVA).

Dystrophin messenger rescue analysis. Total RNA was extracted from muscles with TRIzol reagent (Life Technologies) and treated with RNAse-free DNAse I from the TURBO DNA-free kit (Life Technologies) according to the manufacturer's instructions. Five hundred nanograms of this RNA were reverse transcribed using random primers (Life Technologies) and M-MLV reverse transcriptase (Life Technologies). Detection of the canine dystrophin messenger was done using a nested PCR from exon 3

to 10, using GoTaq DNA polymerase (Promega, Charbonnieres, France) and primers (Life Technologies) and amplification conditions previously described.[15] Final PCR products were migrated on an agarose gel and revealed with ethidium bromide staining.

Immunohistochemistry analysis. Muscles samples were snap-frozen in isopentane cooled in liquid nitrogen and stored at −80 °C until processing. Serial frozen transverse sections 12 µm were cut using a cryostat (Leica Microsystems, Nanterre, France). Transversal cryosections were incubated in blocking buffer (phosphate-buffered saline (PBS)/5% goat serum) for 1 hour at room temperature, and then incubated overnight at room temperature in PBS with mouse monoclonal anti-dystrophin antibody (Novocastra NCL-DYS2, 1:50, Menarini, Rungis, France). The sections were then incubated for 1 hour at room temperature with Alexa fluor 488-conjugated goat anti-mouse IgG (1:400, Life Technologies), then with the fluorescent DNA-dye DRAQ5 (1:1,000, Biostatus, Leicestershire, UK) for 15 minutes at room temperature, and finally washed with PBS before mounting. Immunofluorescence labeling was observed with an epifluorescence microscope (Nikon, Champigny sur Marne, France).

For histomorphometrical counting of the percentage of dystrophin-positive fibers, a goat anti-mouse biotinylated IgG (1:300, Dako, Les Ullis, France) was used as secondary antibody, diluted in PBS with 5% dog serum. The sections were then incubated 1 hour at room temperature with streptavidin/HRP (1:300, Dako), and revealed with 3,3′-diaminobenzidine (DAB, Dako). Statistical analyses were performed using a Fischer's least significant difference test after two-way ANOVA.

Western-blot analysis. For each muscle sample, total proteins were extracted from twenty 10 µm-thick slices using 100 µl of extraction buffer containing 75 mmol/l Tris-HCl, pH 6.8, 15% SDS, 20% glycerol, and protease inhibitors (cOmplete, Mini, ethylenediaminetetraacetic acid-free Protease Inhibitor Cocktail Tablets, Roche). Hundred micrograms of protein extracts were loaded on a 7–4% SDS-PAGE, migrated at 100V overnight at 4 °C and transfer in methanol buffer at 1A during 6 hours at 4 °C on a nitrocellulose membrane (Millipore, Molsheim, France). Coomassie blue staining of the gel evaluated the efficiency of the transfer. After Red Ponceau staining (Sigma-Aldrich, Lyon, France), membranes were blocked in 5% skim milk in Tris-buffered saline buffer and hybridized with two mouse anti-dystrophin antibodies (1:150, Novocastra, NCL-DYS1 and 1:100, NCL-DYS2, Menarini) and with a secondary anti-mouse IgG HRP-conjugated antibody (1:1,000, Dako). Immunoblots were visualized by Immobilon Western Chemiluminescent HRP substrate (Millipore) on ECL-Hyperfilm (GE Healthcare, Velizy-Villacoublay, France).

Histomorphological analysis. Regeneration was evaluated after immunohistochemical revelation of myofibers with an antibody specific of a developmental myosin heavy chain isoform (1:20, Novocastra, NCL-MHCd, Menarini). The percentages of labeled areas were measured after manual threshold on all muscle cross-sections (reproducibility coefficient: 17%). Total and endomysial fibrosis were evaluated after immunohistochemical revelation of collagen I (1:500, MP biomedicals, Illkirch, France). The endomysial areas were selected by the operator, the threshold level was selected and an automatic measurement of the percentage of the labeled area was done. Twenty fields were randomly chosen to finally evaluate the level of endomysial fibrosis in each muscle (reproducibility coefficients: 1% with ×10 magnification for total fibrosis and 7% with ×20 magnification for endomysial fibrosis). All measurements were automatically performed using Nikon's NIS-Elements software (Nikon, Champigny sur Marne, France). Statistical analyses were performed using a Fischer's least significant difference test after two-way analysis of variance.

NMR imaging and spectroscopy analysis. This assessment was done in a blinded fashion, *i.e.*, the operator was not aware of the injected versus the noninjected forelimb. NMR imaging was performed at 3 tesla in a Siemens Magnetom Trio TIM imager/spectrometer (Siemens, Saint-Denis, France) in the injected forelimb and in the noninjected contralateral forelimb, as previously described.[48] Ten significant quantitative indices were calculated from the ^{1}H NMR signal of three different muscles (extensor carpi radialis brevis, extensor carpi radialis longus, and flexor carpi ulnaris). The most relevant NMR imaging indices relying on T2, T1, and proton density weighted image signal intensities (T2w, T1w, PD), *i.e.*, the T2w/PD and T2w/T1w ratios, the T2w heterogeneity and the maximum relative enhancement after intravenous bolus injection of Gadolinium chelate were analyzed. All indices from the muscles of the injected forelimb were compared to those of the noninjected forelimb, and to reference data collected during a previous NMR study of disease progression in a group of untreated GRMD and healthy dogs.[48] The ^{31}P spectroscopy was realized at 4 tesla in a 46-cm free bore magnet (Magnex Scientific, Oxford, UK) interfaced to a Bruker Biospec spectrometer (Bruker Medical Gmbh, Vienna, Austria), with a 2 cm diameter coil collecting signal from the two extensor carpi radialis muscle, also as previously described.[26] Signals were measured from the two extensor carpi radialis muscles. Phosphocreatine (PCr), the β-phosphate of ATP, phospho-mono and -diesters (PDE, PME), and two resonances of inorganic phosphate were measured on ^{31}P spectra, from which 7 ratios and the pH values for both Pi resonances were calculated.[26]

Functional assessment. This assessment was done in a blinded fashion, *i.e.*, the operator was not aware of the injected versus the noninjected forelimb. The flexion and extension strengths of the wrist of the forelimbs were measured using a specific torque measurement device built around interchangeable torquemeters with a nominal scale of either 2 or 20 Nm (Scaime, Annemasse, France). During the experiments, the dogs were anaesthetized using Propofol (Rapinovet, Schering-Plough, MSD, Courbevoie, France) to limit peripheral muscle relaxation.[49] The stimulation of carpal flexors and extensors was performed by direct nerve stimulation using two thin insulated needles (28G, TECA, Viasys Healthcare, Conshohocken, Pennsylvania). The flexion and extension torques were measured during the stimulation of either the median and ulnar common nerve branches or the radial nerve. Stimulation trains were generated during 500 ms at supramaximal intensity and various stimulation frequencies (5, 10, 20, 25, 50, 100, 133, and 200 Hz). Stimuli were biphasic with a total duration of 1ms. Thirty-second rest periods were respected between contractions. For each muscle function (flexion and extension) and each side (injected and control), the value retained to characterize the maximal strength of the dogs was the maximal torque detected over all the elicited tetanic contractions.

Three measurement sessions were performed all along the protocol. The maximal torque was expressed as a percentage of predicted values computed using a model based on control values with respect to the animal weight. The relative slope over the three visits was used as an indicator of strength change for each function and each side. The strength changes were then analyzed with respect to the dystrophin expression measured in the main wrist flexor (averaged over flexor carpi radialis and flexor carpi ulnaris) and extensor (extensor carpi radialis) muscles. Dystrophin expression was classified into three groups: less than 1%, between 1 and 40% and over 40% of dystrophin positive fibers. The effect of dystrophin expression on strength changes was then tested using a nonparametric Kruskal–Wallis test.

SUPPLEMENTARY MATERIAL

Supplementary Materials and Methods: Follow up of the immune responses.

Supplementary References.

Figure S1. Heterogeneity of dystrophin expression pattern between different muscles within a same injected forelimb.

Figure S2. Relationship between the percentage of dystrophin positive fibers and the number vg/dg.

Figure S3. Detection of anti-dystrophin IgG antibodies by Western-Blot in injected dog sera.

Figure S4. Titers of anti-AAV8 IgG, IgM and NAF in the sera of the injected dogs.

Table S1. Characteristics of the different rAAV8-U7nRNA-E6/E8 vector batches used in this study.

Table S2. Muscles and organs sampled in each dog at euthanasia.
Table S3. Vector shedding in urine and serum of the injected dogs.
Table S4. AAV8 capsid and dystrophin specific IFN-γ secretion data from PBMC and splenocytes of dogs.

ACKNOWLEDGMENTS

We thank all the personnel of the Boisbonne Center for Gene Therapy (ONIRIS, Atlantic Gene Therapies, Nantes, France) for the handling and care of the GRMD dog colony. We also thank Peggy Adin-Chabon, Nathalie Lambert, Caroline Burie, Jonathan Lecaille, Julien Blin (Genethon, Evry, France), and Laurence Dubreil (Atlantic Gene Therapies, INRA UMR 703, Nantes, France) for their technical assistance. We thank Karl Rouger (Atlantic Gene Therapies, INRA UMR 703, Nantes, France) for providing GRMD myoblasts used for testing the *in vitro* functionality of our vectors. We thank Stéphane Blot (Veterinary School of Maisons-Alfort, France) for providing anti-dystrophin IgG positive canine sera from immunized GRMD dogs. And we finally thank Fulvio Mavilio (Genethon, Evry, France) for his critical reading of this manuscript. This project was supported by AFM-Téléthon (Association Française contre les Myopathies) and by ADNA (Advanced Diagnostics for New Therapeutic Approaches), a program dedicated to personalized medicine, coordinated by Institut Mérieux and supported by research and innovation aid from the French public agency, Bpifrance.

REFERENCES

1. Moser, H (1984). Duchenne muscular dystrophy: pathogenetic aspects and genetic prevention. *Hum Genet* **66**: 17–40.
2. Rodino-Klapac, LR, Mendell, JR and Sahenk, Z (2013). Update on the treatment of Duchenne muscular dystrophy. *Curr Neurol Neurosci Rep* **13**: 332.
3. Muntoni, F, Torelli, S and Ferlini, A (2003). Dystrophin and mutations: one gene, several proteins, multiple phenotypes. *Lancet Neurol* **2**: 731–740.
4. Aartsma-Rus, A (2012). Overview on DMD exon skipping. *Methods Mol Biol* **867**: 97–116.
5. Echigoya, Y and Yokota, T (2014). Skipping multiple exons of dystrophin transcripts using cocktail antisense oligonucleotides. *Nucleic Acid Ther* **24**: 57–68.
6. Cirak, S, Arechavala-Gomeza, V, Guglieri, M, Feng, L, Torelli, S, Anthony, K *et al.* (2011). Exon skipping and dystrophin restoration in patients with Duchenne muscular dystrophy after systemic phosphorodiamidate morpholino oligomer treatment: an open-label, phase 2, dose-escalation study. *Lancet* **378**: 595–605.
7. Goemans, NM, Tulinius, M, van den Akker, JT, Burm, BE, Ekhart, PF, Heuvelmans, N *et al.* (2011). Systemic administration of PRO051 in Duchenne's muscular dystrophy. *N Engl J Med* **364**: 1513–1522.
8. Mendell, JR, Rodino-Klapac, LR, Sahenk, Z, Roush, K, Bird, L, Lowes, LP *et al.*; Eteplirsen Study Group. (2013). Eteplirsen for the treatment of Duchenne muscular dystrophy. *Ann Neurol* **74**: 637–647.
9. Goemans, N (2013). Drisapersen Efficacy and Safety in Duchenne Muscular Dystrophy: Results of a Phase III, Randomized, Double-Blind, Placebo-Controlled Trial (Study DMD114044). *World Muscle Society Congress: Late breaking news*.
10. Gorman, L, Suter, D, Emerick, V, Schümperli, D and Kole, R (1998). Stable alteration of pre-mRNA splicing patterns by modified U7 small nuclear RNAs. *Proc Natl Acad Sci USA* **95**: 4929–4934.
11. Jiang, H, Pierce, GF, Ozelo, MC, de Paula, EV, Vargas, JA, Smith, P *et al.* (2006). Evidence of multiyear factor IX expression by AAV-mediated gene transfer to skeletal muscle in an individual with severe hemophilia B. *Mol Ther* **14**: 452–455.
12. Goyenvalle, A, Vulin, A, Fougerousse, F, Leturcq, F, Kaplan, JC, Garcia, L *et al.* (2004). Rescue of dystrophic muscle through U7 snRNA-mediated exon skipping. *Science* **306**: 1796–1799.
13. Bish, LT, Sleeper, MM, Forbes, SC, Wang, B, Reynolds, C, Singletary, GE *et al.* (2012). Long-term restoration of cardiac dystrophin expression in golden retriever muscular dystrophy following rAAV6-mediated exon skipping. *Mol Ther* **20**: 580–589.
14. Goyenvalle, A, Babbs, A, Wright, J, Wilkins, V, Powell, D, Garcia, L *et al.* (2012). Rescue of severely affected dystrophin/utrophin-deficient mice through scAAV-U7snRNA-mediated exon skipping. *Hum Mol Genet* **21**: 2559–2571.
15. Vulin, A, Barthélémy, I, Goyenvalle, A, Thibaud, JL, Beley, C, Griffith, G *et al.* (2012). Muscle function recovery in golden retriever muscular dystrophy after AAV1-U7 exon skipping. *Mol Ther* **20**: 2120–2133.
16. Barbash, IM, Cecchini, S, Faranesh, AZ, Virag, T, Li, L, Yang, Y *et al.* (2013). MRI roadmap-guided transendocardial delivery of exon-skipping recombinant adeno-associated virus restores dystrophin expression in a canine model of Duchenne muscular dystrophy. *Gene Ther* **20**: 274–282.
17. Kornegay, JN, Bogan, JR, Bogan, DJ, Childers, MK, Li, J, Nghiem, P *et al.* (2012). Canine models of Duchenne muscular dystrophy and their use in therapeutic strategies. *Mamm Genome* **23**: 85–108.
18. Sharp, NJ, Kornegay, JN, Van Camp, SD, Herbstreith, MH, Secore, SL, Kettle, S *et al.* (1992). An error in dystrophin mRNA processing in golden retriever muscular dystrophy, an animal homologue of Duchenne muscular dystrophy. *Genomics* **13**: 115–121.
19. Su, LT, Gopal, K, Wang, Z, Yin, X, Nelson, A, Kozyak, BW *et al.* (2005). Uniform scale-independent gene transfer to striated muscle after transvenular extravasation of vector. *Circulation* **112**: 1780–1788.
20. Toromanoff, A, Chérel, Y, Guilbaud, M, Penaud-Budloo, M, Snyder, RO, Haskins, ME *et al.* (2008). Safety and efficacy of regional intravenous (r.i.) versus intramuscular (i.m.) delivery of rAAV1 and rAAV8 to nonhuman primate skeletal muscle. *Mol Ther* **16**: 1291–1299.
21. Arruda, VR, Stedman, HH, Haurigot, V, Buchlis, G, Baila, S, Favaro, P *et al.* (2010). Peripheral transvenular delivery of adeno-associated viral vectors to skeletal muscle as a novel therapy for hemophilia B. *Blood* **115**: 4678–4688.
22. Fan, Z, Kocis, K, Valley, R, Howard, JF, Chopra, M, An, H *et al.* (2012). Safety and feasibility of high-pressure transvenous limb perfusion with 0.9% saline in human muscular dystrophy. *Mol Ther* **20**: 456–461.
23. Nguyen, F, Cherel, Y, Guigand, L, Goubault-Leroux, I and Wyers, M (2002). Muscle lesions associated with dystrophin deficiency in neonatal golden retriever puppies. *J Comp Pathol* **126**: 100–108.
24. Dubowitz, V and Sewry, C (2007). Duchenne and Becker muscular dystrophy. In: *Muscle Biopsy: A Practical Approach*, 3rd edn. Elsevier: Philadelphia. pp. 297–304.
25. Thibaud, JL, Monnet, A, Bertoldi, D, Barthélémy, I, Blot, S and Carlier, PG (2007). Characterization of dystrophic muscle in golden retriever muscular dystrophy dogs by nuclear magnetic resonance imaging. *Neuromuscul Disord* **17**: 575–584.
26. Wary, C, Naulet, T, Thibaud, JL, Monnet, A, Blot, S and Carlier, PG (2012). Splitting of Pi and other ^{31}P NMR anomalies of skeletal muscle metabolites in canine muscular dystrophy. *NMR Biomed* **25**: 1160–1169.
27. Yokota, T, Lu, QL, Partridge, T, Kobayashi, M, Nakamura, A, Takeda, S *et al.* (2009). Efficacy of systemic morpholino exon-skipping in Duchenne dystrophy dogs. *Ann Neurol* **65**: 667–676.
28. Yokota, T, Nakamura, A, Nagata, T, Saito, T, Kobayashi, M, Aoki, Y *et al.* (2012). Extensive and prolonged restoration of dystrophin expression with vivo-morpholino-mediated multiple exon skipping in dystrophic dogs. *Nucleic Acid Ther* **22**: 306–315.
29. Neri, M, Torelli, S, Brown, S, Ugo, I, Sabatelli, P, Merlini, L *et al.* (2007). Dystrophin levels as low as 30% are sufficient to avoid muscular dystrophy in the human. *Neuromuscul Disord* **17**: 913–918.
30. Anthony, K, Cirak, S, Torelli, S, Tasca, G, Feng, L, Arechavala-Gomeza, V *et al.* (2011). Dystrophin quantification and clinical correlations in Becker muscular dystrophy: implications for clinical trials. *Brain* **134**(Pt 12): 3547–3559.
31. Sharp, PS, Bye-a-Jee, H and Wells, DJ (2011). Physiological characterization of muscle strength with variable levels of dystrophin restoration in mdx mice following local antisense therapy. *Mol Ther* **19**: 165–171.
32. van Putten, M, Hulsker, M, Nadarajah, VD, van Heiningen, SH, van Huizen, E, van Iterson, M *et al.* (2012). The effects of low levels of dystrophin on mouse muscle function and pathology. *PLoS ONE* **7**: e31937.
33. Banks, GB and Chamberlain, JS (2008). The value of mammalian models for duchenne muscular dystrophy in developing therapeutic strategies. *Curr Top Dev Biol* **84**: 431–453.
34. Niemeyer, GP, Herzog, RW, Mount, J, Arruda, VR, Tillson, DM, Hathcock, J *et al.* (2009). Long-term correction of inhibitor-prone hemophilia B dogs treated with liver-directed AAV2-mediated factor IX gene therapy. *Blood* **113**: 797–806.
35. Bartoli, M, Poupiot, J, Goyenvalle, A, Perez, N, Garcia, L, Danos, O *et al.* (2006). Noninvasive monitoring of therapeutic gene transfer in animal models of muscular dystrophies. *Gene Ther* **13**: 20–28.
36. Le Hir, M, Goyenvalle, A, Peccate, C, Précigout, G, Davies, KE, Voit, T *et al.* (2013). AAV genome loss from dystrophic mouse muscles during AAV-U7 snRNA-mediated exon-skipping therapy. *Mol Ther* **21**: 1551–1558.
37. Nowrouzi, A, Penaud-Budloo, M, Kaeppel, C, Appelt, U, Le Guiner, C, Moullier, P *et al.* (2012). Integration frequency and intermolecular recombination of rAAV vectors in non-human primate skeletal muscle and liver. *Mol Ther* **20**: 1177–1186.
38. Schmidt, WM, Uddin, MH, Dysek, S, Moser-Thier, K, Pirker, C, Höger, H *et al.* (2011). DNA damage, somatic aneuploidy, and malignant sarcoma susceptibility in muscular dystrophies. *PLoS Genet* **7**: e1002042.
39. Colussi, C, Gurtner, A, Rosati, J, Illi, B, Ragone, G, Piaggio, G *et al.* (2009). Nitric oxide deficiency determines global chromatin changes in Duchenne muscular dystrophy. *FASEB J* **23**: 2131–2141.
40. Wu, B, Cloer, C, Lu, P, Milazi, S, Shaban, M, Shah, SN *et al.* (2014). Exon skipping restores dystrophin expression, but fails to prevent disease progression in later stage dystrophic dko mice. *Gene Ther*. doi: 10.1038/gt.2014.53 [Epub ahead of print].
41. Toromanoff, A, Adjali, O, Larcher, T, Hill, M, Guigand, L, Chenuaud, P *et al.* (2010). Lack of immunotoxicity after regional intravenous (RI) delivery of rAAV to nonhuman primate skeletal muscle. *Mol Ther* **18**: 151–160.
42. Haurigot, V, Mingozzi, F, Buchlis, G, Hui, DJ, Chen, Y, Basner-Tschakarjan, E *et al.* (2010). Safety of AAV factor IX peripheral transvenular gene delivery to muscle in hemophilia B dogs. *Mol Ther* **18**: 1318–1329.
43. Sherratt, TG, Vulliamy, T, Dubowitz, V, Sewry, CA and Strong, PN (1993). Exon skipping and translation in patients with frameshift deletions in the dystrophin gene. *Am J Hum Genet* **53**: 1007–1015.
44. Mendell, JR, Campbell, K, Rodino-Klapac, L, Sahenk, Z, Shilling, C, Lewis, S *et al.* (2010). Dystrophin immunity in Duchenne's muscular dystrophy. *N Engl J Med* **363**: 1429–1437.
45. Flanigan, KM, Campbell, K, Viollet, L, Wang, W, Gomez, AM, Walker, CM *et al.* (2013). Anti-dystrophin T cell responses in Duchenne muscular dystrophy: prevalence and a glucocorticoid treatment effect. *Hum Gene Ther* **24**: 797–806.
46. Smith, RH, Levy, JR and Kotin, RM (2009). A simplified baculovirus-AAV expression vector system coupled with one-step affinity purification yields high-titer rAAV stocks from insect cells. *Mol Ther* **17**: 1888–1896.
47. Le Guiner, C, Moullier, P and Arruda, VR (2011). Biodistribution and shedding of AAV vectors. *Methods Mol Biol* **807**: 339–359.
48. Thibaud, JL, Azzabou, N, Barthelemy, I, Fleury, S, Cabrol, L, Blot, S *et al.* (2012). Comprehensive longitudinal characterization of canine muscular dystrophy by serial NMR imaging of GRMD dogs. *Neuromuscul Disord* **22** (suppl. 2): S85–S99.
49. Dueck, MH, Oberthuer, A, Wedekind, C, Paul, M and Boerner, U (2003). Propofol impairs the central but not the peripheral part of the motor system. *Anesth Analg* **96**: 449–55, table of contents.
50. Reiss, J and Rininsland, F (1994). An explanation for the constitutive exon 9 cassette splicing of the DMD gene. *Hum Mol Genet* **3**: 295–298.